Fabrication of In-Channel High-Aspect Ratio Sensing Pillars for Protrusive Force Measurements on Fungi and Oomycetes

Yiling Sun, *Member, IEEE*, Ayelen Tayagui, Ashley Garrill, and Volker Nock, *Member, IEEE*

***Abstract*— This paper reports the fabrication and application of a Lab-on-a-Chip platform containing single-elastomeric micropillars in channel constrictions, which enable the measurement of protrusive forces exerted by individual fungal hyphae. We show the device design, the fabrication process, and photoresist optimization required to adapt the microfluidic platform to relatively thin hyphae. To demonstrate the applicability of the devices, the oomycete *Achlya bisexualis* and the fungus *Neurospora crassa* were cultured on PDMS chips. Devices were combined with confocal imaging to study the interaction of *A. bisexualis* hyphae with the measurement pillars. The force exerted by individual hyphae of *N. crassa* was measured and compared with a hyphal growth rate and diameter. The platform provides a new tool to help understand the molecular processes that underlie protrusive growth and this may present new ways to tackle the pathogenic growth of these organisms and thus combat the loss of diversity that they cause. This paper is based on the conference proceedings presented at the 31st IEEE International Conference on Micro Electro Mechanical Systems (MEMS 2018), Belfast. [2018-0090]**

***Index Terms*— Lab-on-a-chip, force sensor, PDMS micropillars, fungi and oomycetes.**

I. Introduction

FUNGI and oomycete are crucial components of most ecosystems, playing a key role in the breakdown of organic matter and nutrient recycling. However, some species have the potential to be pathogenic and can cause significant disease to plants and animals [2]. Indeed, some of the most severe die-offs and extinctions have been caused by these organisms. Relevant examples include the white nose disease of bats, the snake die-off disease and chytridiomycosis in amphibians [3], [4]. This is compounded by the fact that an increasing number of pathogenic fungi are developing resistance to antifungal drugs, thus challenging human health and food security [5]. In many cases pathogenic growth involves the invasive penetration of host tissue by individual hyphae which extend by the process of tip growth [6]. This is driven by the internal hydrostatic pressure (turgor) of the hyphae [7], [8]. Yielding of the hyphal tip to this pressure enables the generation of a protrusive force [9]. In order to begin to understand the molecular mechanisms that underlie invasive tip growth it is important to be able to measure this protrusive force [10]. Previous measurements of protrusive forces exerted by single hyphae have been made using a miniature silicon bridge strain gauge [11]. The forces were measured in proportion to deformation of the silicon beam when hyphae grew against the strain gauge. However, experiments with strain gauges are complicated because the silicon beam of the device is 0.1 *mm* thick and 10 *mm* wide, in comparison the diameter of a fungal hypha is typically less than 30 micrometers. More recently, Lab-on-a-Chip (LoC) devices have been used in biomechanical studies on tip-growing cells [12], [13]. Despite the number of existing platforms, reports on the characterization and sensing methods of invasive growth forces exerted by tip-growing cells are scarce. A polydimethylsiloxane (PDMS) array containing 10,000 cylindrical microchambers was devised as a force sensor for single cells of rod-shaped fission yeast *Schizosaccaromyces pombe* [14]. Single fission yeast cells were introduced into chambers and as they extended they pushed against the wall of chambers. Similarly, based on the deformation of elastic PDMS, a microfluidic device with narrow gaps in channels was developed [15]. Pollen tubes grew through the channels with an array of narrow gaps, applying a penetrative force deforming the sidewalls of the gap. Due to the geometry, this system measures squeezing forces rather than protrusive forces due to different contact points of obstacles. Based on devices that were originally designed to study nematode movements [16], [17], we have recently reported the use of elastomeric micropillars as a platform technology for the study of protrusive forces generated in hyphae [1], [18]–[20]. The current work extends this by optimizing the fabrication and photolithography in order to decrease the sensor pillar diameter and channel-pillar gap from dimensions used with the oomycete *Achlya bisexualis*, to make the platform suitable for use with fungi with thinner hyphae, such as the model organism *N. crassa* [21]. To demonstrate the applicability of the platform, we used the devices to characterize the

Manuscript received April 22, 2018; revised July 4, 2018; accepted July 27, 2018. Date of publication August 16, 2018; date of current version October 1, 2018. This work was supported in part by Marsden under Grant UOC1504, in part by the Brian Mason Trust, and in part by the Biomolecular Interaction Centre. Subject Editor J. A. Yeh. *(Corresponding author: Volker Nock.)*

Y. Sun and V. Nock are with the Department of Electrical and Computer Engineering, University of Canterbury, Christchurch 8140, New Zealand (e-mail: volker.nock@canterbury.ac.nz).

A. Tayagui and A. Garrill are with the School of Biological Sciences, University of Canterbury, Christchurch 8140, New Zealand.

This paper has supplementary downloadable material available at http://ieeexplore.ieee.org provided by the authors.

Color versions of one or more of the figures in this paper are available online at http://ieeexplore.ieee.org.

Digital Object Identifier 10.1109/JMEMS.2018.2862863

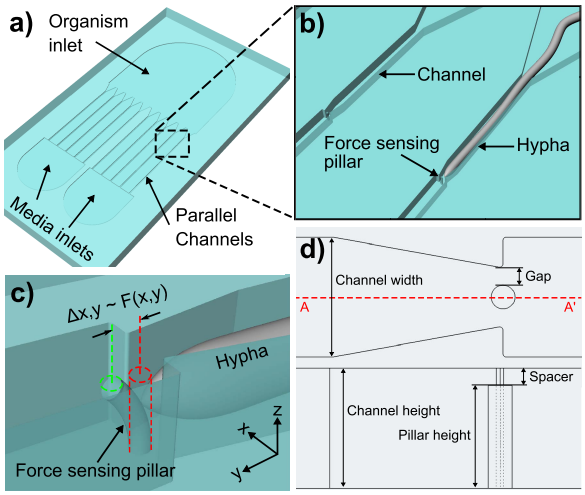

Fig. 1. Design of the force sensing platform. (a) Entire chip showing the geometry of the device with a common seeding area (organism inlet) and parallel measurement channels connected to separate media inlets. (b) Single channels are used to isolate individual hyphae and guide them against an elastomeric force-sensing pillar. (c) Hyphal contact with the force-sensing pillar causes a translation of the pillar top. This translation $\Delta x, y$ is converted into force magnitude and direction $F(x, y)$ via image processing and a mechanical deflection model. (d) Sketch of a typical pillar constriction indicating the horizontal and vertical gaps between the pillar and the wall, and the pillar and the lid, respectively. To increase comparability and measurement accuracy, the spacer and gap need to be minimized during fabrication, while maintaining a pillar/channel height suitable for the size of the target organism.

interaction of *A. bisexualis* hyphae with measurement pillars using confocal microscopy and recorded force measurements of multiple hyphae of *N. crassa*.

II. Experimental

A. Chip Design

The microfluidic device is comprised of twelve parallel measurement channels, each with an integrated, freely-bending single elastomeric micropillar as a force sensor. Measurement channels connect a seeding area for cell inoculation and two media inlets for media supply and independent chemical stimulation (see Fig. 1). Fungal hyphae grow out from the seeding area into the channels and deflect the force-sensing micropillars. The width of leading edge *A. bisexualis* and *N. crassa* hyphae are typically between 18 - 30 μm and 8 - 15 μm, respectively. Therefore, the width of the channels were set to 35 and 15 μm, respectively, thus allowing only single hyphae to grow into them. The heights of micropillars were set to 25 and 12 μm, respectively. A spacer layer, 5 or 3 μm in height, was included to prevent the pillar top from touching the channel lid, resulting in free bending [20]. While smaller diameter micropillars in general mean higher sensitivity force sensing, due to photolithographical considerations we limited pillars sizes to 5 and 7 μm in diameter in the current design.

B. Chip Fabrication

The microfluidic PDMS chip was fabricated by replica-molding off a two-layer resist master, which provides a vertical gap between the top of micropillar and channel lid by use of a spacer layer, as shown in Fig. 2. Due to diffraction and refraction effects of UV light, it was difficult to produce high aspect-ratio pillar cavities using negative photoresist. A combination

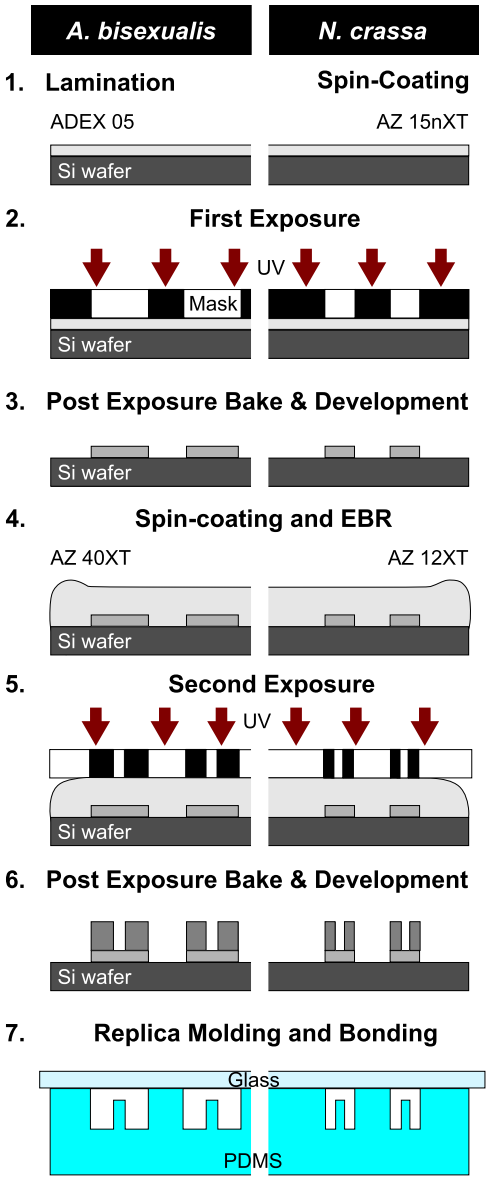

Fig. 2. Fabrication process of the PDMS devices for *A. bisexualis* (left) and *N. crassa* (right). Due to the difference in organism size, two different photoresist combinations had to be used to fabricate the mold masters. (1-3): Depending on the target organism, dry film ADEX 05 photoresist was laminated or AZ 15nXT (115 CPS) spin-coated and processed to form the spacer layer. (4-6): Positive resist AZ 40XT or AZ 12XT were then spin-coated and processed to form the respective pillar layer. (7): Replica-cast PDMS chips were sealed onto glass coverslips with pre-drilled access holes or fluorodishes for confocal microscopy.

of negative and positive photoresists were therefore employed to build an integrated mold with high-aspect pillar cavity inside a channel constriction. In the following, we describe the process parameters for devices aimed at both, *A. bisexualis* and *N. crassa* to compare the difference in dimensions and thus process optimization required to produce devices for fungi with increasingly thinner hyphae.

In brief, two 4″ chrome-on-glass photomasks (Nanofilm) were prepared using a tabletop micro pattern generator (μPG101, Heidelberg Instruments). The first-layer mask contained the channel outlines, seeding area and inlets, while the

second-layer mask contained the same features with the addition of measurement pillar outlines. Depending on the channel and pillar dimensions of the chips, different combinations of two negative photoresist ADEX 05 (dry-film, thickness 5 μm, DJ Microlaminates) and AZ 15nXT (115 CPS, M.M.R.C Pty Ltd.), and two positive photoresist AZ 40XT and AZ 12XT (M.M.R.C Pty Ltd.) were utilized. A 4″ silicon wafer, 525 μm thickness, was dehydrated in a 185 °C oven for over 2 hours and cleaned by oxygen plasma (K1050X, Emitech) for 10 min at 100 W. A negative photoresist, ADEX 05, or AZ 15nXT, was coated onto the pre-treated silicon wafer by lamination [20] or spin-coating (5000 rpm, 30 sec). The negative resist was then exposed using the first-layer mask by the UV lithography system in vacuum-contact mode. The wafer was developed in propyleneglycol-monomethyletheracetate, rinsed with isopropyl alcohol (IPA) and dried by N_2, followed by a ramped post-exposure bake (PEB). The second layer of the positive photoresist (AZ 40XT or AZ 12XT) was spin-coated onto the first spacer layer resist (2000 rpm for AZ 40XT reaching a thickness of 24 μm, or 1500 rpm for AZ 12XT with a final thickness of 11 μm). After edge-bead removal (EBR) using AZ EBR solvent and soft-baking on a hotplate, the positive resist was exposed using the second layer mask. After PEB, the resist master mold was completed by development in resist developer (AZ 326MIF, M.M.R.C Pty Ltd.), rinsed with IPA and dried by N_2.

The PDMS chip was molded from Sylgard 184 silicone elastomer (Dow Corning, 10:1 w/w). First, the master mold was treated by vapor-coating with Trichloro(1H,1H,2H, 2H-perfluorooctyl) silane (TFOCS, Sigma-Aldrich) in a desiccator for 30 min to facilitate mold release. Then, pre-mixed PDMS was poured onto the treated mold and degassed until all bubbles had disappeared (> 30 min). After a 2 hour bake at 80 °C on a hotplate, the PDMS chip was peeled off carefully and placed on a hotplate for an additional 4 hour bake at 80 °C to ensure the PDMS was completely cured. Glass covers were prepared by drilling holes into a glass microscope slide (VWR) using a 3 mm-diameter diamond-coated hole drill (28.5030, Esslinger) and cleaned in a sequence of acetone, methanol and IPA for 5 min each. The microfluidic chip was finished by manually aligning and bonding the PDMS chip with the glass substrate using 30 s exposure to 100 W oxygen plasma in a barrel asher (K1050X, Emitech) and baking for 2 hours at 80 °C. Fabricated microfluidic chips were degassed for 2 hours in a vacuum chamber to improve filling with media and sealed into food-grade vacuum bags using a vacuum sealer (Sunbeam FoodSaver).

C. Experimental Setup

The PDMS chips aimed at *A. bisexualis* force measurement was promptly filled with peptone yeast glucose broth (PYG, containing [in % w/v] peptone [0.125], yeast extract [0.125] and glucose [0.3]) once taken out from the sealed vacuum package. The oomycete *A. bisexualis* was cultured on PYG agar Petrie dish (containing [in % w/v] peptone [0.125], yeast extract [0.125], glucose [0.3], and agar [2]) for 48 hours. An inoculation plug of *A. bisexualis* (3 mm in diameter) was cut from the culture growing edge and transferred to the seeding area of the platform. Hyphae were then observed to grow from the seeding area into the measurement channels.

In terms of the PDMS chips for *N. crassa*, they were filled with Vogel's broth (containing [in % w/v] sucrose [1.5] and 2 mL of Vogels 50X salt solution). Stock cultures of fungi *N. crassa* were grown on Vogels media (containing [in % w/v] sucrose [1.5], agar [1.5] and 2 mL of Vogels 50X salt solution) for 24 h at 26 °C. A 2.5 mm diameter inoculation plug was cut from the edge of a stock culture using a biopsy punch and then transferred to the seeding area of the chip. Hyphae were left to grow from the seeding area into the channels. At 26 °C it took them around 6 h to reach the pillars.

Once the hyphae grew close to the force-sensing pillars, pillar deflection by the tip of each hypha was recorded using a light microscope (Nikon Eclipse 80i) with digital camera (ORCA-Flash4.0 V2, Hamamatsu). The force exerted by hyphae was calculated by a combination of image processing for tracking in ImageJ (V1.51u, FIJI) [22] and analysis in MATLAB (2017b, Mathworks). A custom image-processing algorithm implemented in MATLAB was used in conjunction with pre-calibrated mechanical pillar properties to convert the measured deflection into force values [20].

For confocal imaging of *A. bisexualis*, PDMS devices were plasma-bonded to fluorodishes (FD35-100, WPI Inc.) as described above. Instead of glass drilling, inlet and outlet holes were punched through the PDMS using a 3 mm diameter hole punch before bonding. PYG broth on the chip was replaced with PYG containing tartrazine (trisodium 1-(4-sulfonatophenyl)-4-(4-sulfonatophenylazo)-5-pyrazolone-3-carboxylate)), which is a synthetic lemon-yellow dye that is commonly used as a food colouring (E102). The tartrazine was bought as Hansells Yellow Colouring (Hansells Food Group, Auckland, NZ) and obtained from a local supermarket. Solutions on the chips were changed using a perfusion method. This was done by first removing some of the PYG broth from the seeding area on the chip using a pipette (5 μl of dye was added, assuming the total volume of the chip was 40 μl) and then adding the dye solution to the media supply port. As they were close to the pillars, the hyphal tips were closer to the media supply port than the seeding area. Also, the added solution was expelled with force from the tip of the pipette such the solution reached the growing tip of a hypha mostly by convectional flow, rather than just by simple diffusion. All subsequent solution changes were done using this perfusion technique. Hyphae and pillars were then imaged with a confocal microscope (Leica TCS SP5) using the 63x (NA 1.3) glycerol objective lens. Tartrazine was excited using the argon laser at 488 nm with 30% intensity with an emission bandwidth of 502-605 nm. The fluorescence was detected concurrently with transmitted light images collected with bright field optics. Data was analyzed using the 5D Viewer plug-in of ImageJ (V1.51u, FIJI) [22].

III. Results and Discussion

Elastomeric micropillars represent a versatile platform technology for the study of protrusive forces generated

by hyphal organisms. The ability to measure forces by simply tracking the deflection of pillars inside otherwise transparent microfluidic devices makes the technology well suited for adoption in biological research. In comparison to other pillar-based techniques, such as magnetic [23] or microelectromechanical [24], [25] force transduction, the devices presented here only require a conventional optical microscope for sensor read-out, which is a common tool found in microbiology laboratories. However, the successful measurement of protrusive forces exerted by hyphae requires the monolithic integration of high-aspect ratio elastomeric micropillars into microfluidic channels via replica-casting of a multi-layer mold. To prevent hyphae from avoiding the pillars, these have to be placed as close to the channel walls as possible [18]. Traditional methods involve the fabrication of master structures from silicon. However, these are expensive and complex for multi-level high-aspect-ratio microstructures. SU-8 negative resist masters represent a less expensive alternative to silicon, but the fabrication of SU-8 molds with negative microstructures (deep cavities) is difficult due to lack of exchange of fresh SU-8 developer in micro-cavities [26].

PDMS double-casting can reduce some of these challenges by allowing one to invert the geometry from cavities to pillars on the mold. However, we found the yield of this process insufficient (data not shown) to produce device quantities needed for biologically-relevant sample sizes. In case of the work presented here, the cavity problem is also compounded by the device design and the mask polarity required for a negative resist such as SU-8. Integrated individual pillars require large open areas (channel outline) next to small opaque features (pillar cavity), which limits the available exposure window. This in particular becomes a lithographically simpler problem when positive tone resists can be used. To retain the low-cost approach of a photoresist mold we thus developed a process combining a negative resist for the spacer layer and a positive resists for the pillar layer on the same mold to produce a monolithic mold master. In case of devices for use with *A. bisexualis*, we combined ADEX 05 as negative resist (spacer layer) with AZ 40XT positive resist (pillar layer). For *N. crassa* devices we combined AZ 15NXT as negative resist (spacer layer) with AZ 12XT positive resist (pillar layer) to reduce the device dimensions in response to the smaller organism size.

Due to the relative novelty of the positive photoresists AZ 40XT and AZ 12XT, and negative photoresist AZ 15NXT, used in this work, little information exists on their processing. Thus, the exposure latitude of the positive photoresists was characterized in combination with the subjacent negative resist by measuring the widths of channels and diameters of pillar cavities (5 and 7 μm) for various exposure doses. First, an exposure dose trial ranging from 200 to 350 mJ/cm^2, was carried out for the photoresist AZ 40XT (see Fig. 3), with the negative photoresist ADEX 05 acting as the first channel layer as reported previously [20]. Figure 3(a) shows the plot of the dose trial results for the photoresist AZ 40XT (24 μm in thickness), as used for *A. bisexualis* chips. The dots (blue) represent the mean width of 8 channels, and diamond (gray) and triangle (orange) are the mean diameters of cavities

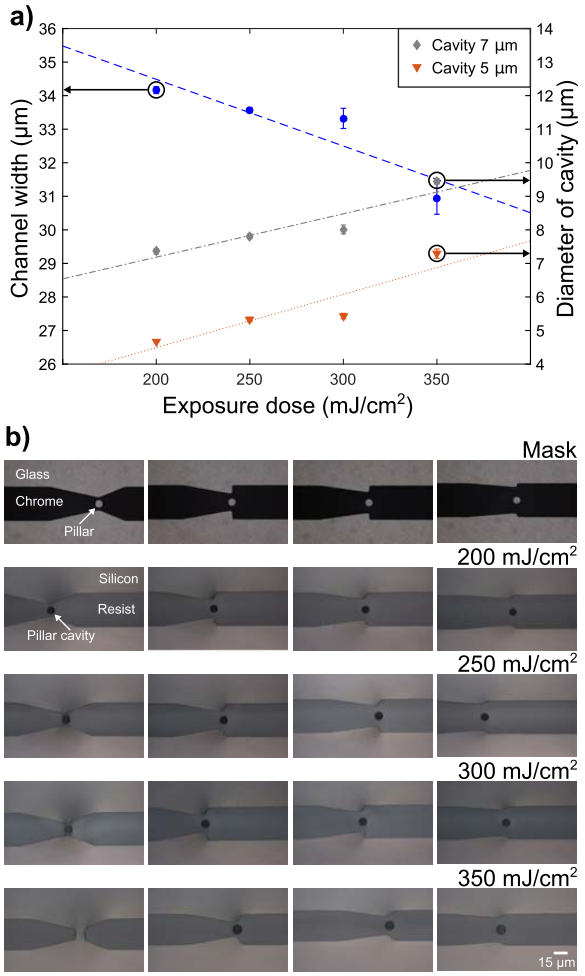

Fig. 3. Dose trial results for the positive-tone photoresist AZ 40XT used for layer two of the *A. bisexualis* chip with a thickness of 24 μm. (a) Plot of the channel width and diameter of pillar cavity as a function of exposure dose. Two different pillar cavity diameters of 5 and 7 μm were included on the mask. (b) Optical micrographs of four different constriction geometries with 7 μm pillar cavity diameter and gap size between the cavity and channel wall increasing from 3, 5, 7 to 10 μm gap from left to right. The top row shows the mask design and the following rows the resulting resist pattern in AZ 40XT at an exposure dose of 200, 250, 300 and 350 mJ/cm^2, respectively. It can be observed that the pillar cavity diameter increases with exposure dose (top to bottom rows) and that the narrowest gap of 3 μm (left column) cannot be resolved at exposure doses higher than 250 mJ/cm^2.

7 and 5 μm, respectively. For both patterns, the diameter of cavities was found to increase with exposure dose from 4.7 to 7.3 μm, and 7.4 to 9.4 μm, respectively, while the width of the channel decreased, ranging from 34.2 to 30.9 μm. The channels and pillar cavities on the mask were measured as 34.5 μm in width, 6.9 and 4.7 μm in diameter. The corresponding optical micrographs of resist patterns are shown in Fig. 3(b) for four different constriction designs and as a function of exposure dose. The pillar cavity diameter was found to increase with exposure dose, while the narrowest pillar-wall gap of 3 μm could not be resolved at exposure doses higher than 250 mJ/cm^2.

Next, negative-tone photoresist AZ 15nXT was characterized for its ability to replicate the channel structure in the spacer layer for *N. crassa* devices. Three different exposure

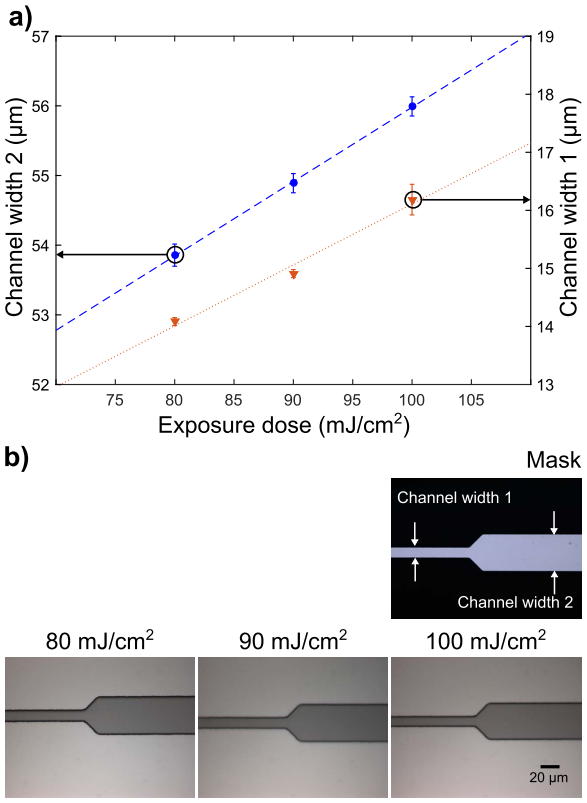

Fig. 4. Dose trial results for the negative-tone photoresist AZ 15nXT (115CPS) used for layer one of the *N. crassa* chip with a thickness of 2.6 μm. (a) Plot of the channel width before (Channel width 1) and after (Channel width 2) the pillar constriction as a function of exposure power. (b) Optical micrographs of the mask and resulting resist pattern in AZ 15nXT (115CPS) at exposure doses of from left to right 80, 90, 100 mJ/cm^2.

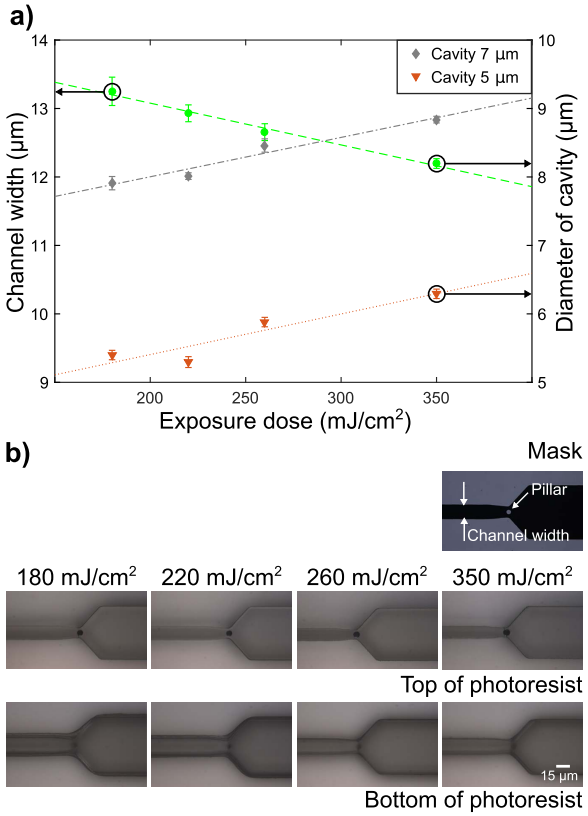

Fig. 5. Dose trial results for the negative-tone photoresist AZ 12XT used for layer two of the *N. crassa* chip with a thickness of 11 μm. (a) Plot of channel width and diameter of pillar cavity as a function of exposure dose. Two different pillar cavity diameters of 5 and 7 μm were included on the mask. (b) Optical micrographs of the mask with 7 μm cavity diameter and resulting resist pattern in AZ 12XT at exposure doses of from left to right 180, 220, 260 and 350 mJ/cm^2. Images in the middle row are focused on the top and images in the bottom row on the bottom of the photoresist. As can be observed, pillar diameter and verticality increase with exposure dose.

doses (80, 90, 100 mJ/cm^2) were trialled for AZ 15nXT resist spin-coated to a thickness of 2.6 μm. Figure 4 shows the plot of the dose trial results and channel micrographs for the photoresist AZ 15nXT. The narrow side before the pillar constriction connecting with seeding area was defined as Channel width 1 and the wide side after the pillar constriction connecting with media inlet was defined as Channel width 2 (see Fig. 4(b). The dots (blue) represent the mean width of Channel width 1, while the triangles (orange) are the mean width of Channel width 2. For both channel width 1 and 2 the measured width increased with increase of exposure dose from 53.9 to 56.0 μm and 14.0 to 16.2 μm, respectively, as is typical for negative-tone photoresists [27].

Similarly as for the combination of AZ 40XT with ADEX 05, exposure doses from 180 to 350 mJ/cm^2 were trialled for the photoresist AZ 12XT with the pre-processed negative photoresist AZ 15nXT coated to a thickness of 2.6 μm as the first layer. It was found that the AZ 12XT was not completely removed after development when exposed to the lower power UV light. At lower exposure doses (180, 220 mJ/cm^2) the widths of the channel outline also varied over the height of the resist, decreasing from top to bottom and indicating non-vertical side walls (see Fig. 5(b)). The overall results of the dose trial for the photoresist AZ 12XT with 11 μm in thickness are plotted in Fig. 5. The dots (green) represent the mean width of 6 channels, and diamonds (gray) and triangles (orange) represent the mean diameters of the 7 and 5 μm cavities, respectively. For both patterns the diameters of the cavities increased with exposure dose from 5.4 to 6.3 μm, and 7.9 to 8.8 μm, respectively. Simultaneously, the widths of channels decreased from 13.3 to 12.2 μm. For comparison, the measured results on the mask were 14.7 μm in width, and 6.9 and 4.3 μm in pillar diameter.

Optimized processing parameters obtained from the dose trials were subsequently used to fabricate devices for use with either *A. bisexualis* or *N. crassa*. Figure 6 shows the PDMS microfluidic chips fabricated using the dual-photoresist molds. The basic design for either organism incorporates a single seeding area and two media inlets connected to the seeding area via six parallel measurement channels each. These inlet channels could be supplied separately with nutrients and/or inhibitors allowing one to measure six samples each per inlet, as shown in Fig. 6(a). Alternatively, inlets could also be combined to increase the number of parallel measurement channels to twelve for one input (see Fig. 6(c)). Externally, the chips could either be connected with tubes from the side to actively provide media exchange, or this can be done

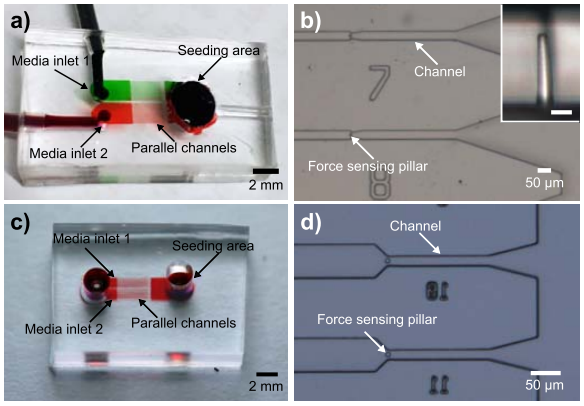

Fig. 6. Devices fabricated using the dual-photoresist mold process. (a) Photograph of a PDMS device for *A. bisexualis*. The design incorporates a combined organism seeding area and two media inlets connected to the seeding area via six parallel measurement channels each. Inlet channels were filled with red and green dye for visualization. (b) Optical micrograph of two measurement channels indicating the location of the force sensing pillars. Inset shows a side-view of a typical PDMS measurement pillar used for *A. bisexualis*. Inset scale bar is 10 μm. (c) Photograph of a PDMS device for *N. crassa*. The design incorporates a combined organism seeding area and two media inlets connected to the seeding area via six parallel measurement channels each. This example shows both inlet channels filled with red dye for visualization and used in parallel via a single inlet hole. (d) Optical micrograph of two measurement channels on the *N. crassa* device indicating the location of the force sensing pillars.

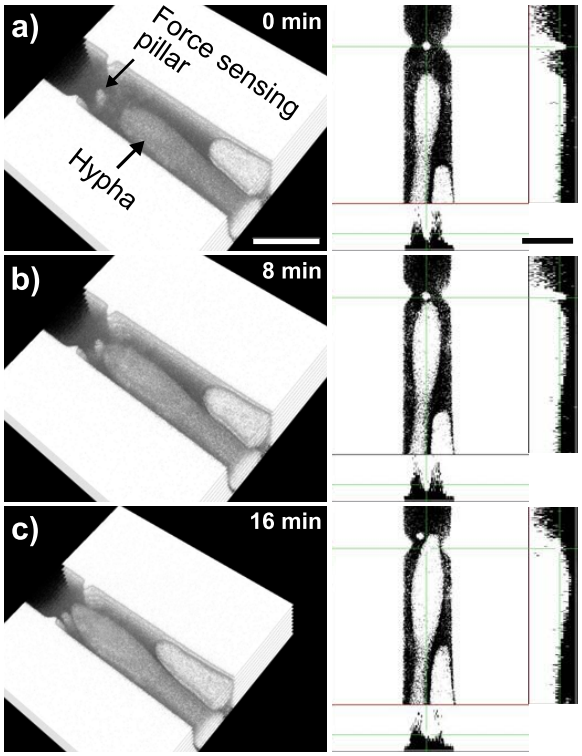

Fig. 7. Confocal microscopy time-series of an *A. bisexualis* a single hypha deflecting a sensor pillar. (a) A hypha extending down a measurement channel filled with fluorescein sodium towards a force sensing pillar, while a second hypha can be seen following the first. The 3D rendering of the event is shown on the left (data inverted), top-view and cross-sections are shown on the right. Scale bar for all images is 35 μm. (b) The leading hypha touches the pillar and applies protrusive force, increasing its diameter in the process. (c) The hypha then deflects off the pillar and proceeds to squeeze through the gap between the pillar and the channel wall, bending the pillar in the process. During the whole event the leading hypha remains in the same plane, indicating that no or only minimal forces are imparted in the vertical direction.

passively by coring a common inlet overlapping with both. As demonstrated by the infusion of colored water in Fig. 6(a), both inlets could be used to set up discrete concentration gradients for comparative studies. Channel designs trialled included continuous-width channels (Fig. 6(b)) and such that have tapered expansions after the pillar constriction (Fig. 6(d)). An example high-aspect ratio force-sensing micropillar used for *A. bisexualis*, with a diameter of 7 μm and a height of 24 μm with the spacer gap above it, is shown as inset in Fig. 6(b).

To demonstrate the applicability of the platform we performed imaging and force measurement experiments on hyphae of both organisms. After using the platform previously to characterize the protrusive forces exhibited by *A. bisexualis* hyphae and the relationship between hyphal diameter and force magnitude [20], we used the optimized devices to demonstrate confocal imaging of hyphal tip - pillar interactions. In view of the role the cytoskeleton likely plays in the generation of protrusive force [9], [28]–[31], it is important that the platform is compatible with high-resolution and high-contrast imaging techniques such as confocal microscopy. The images shown in Fig. 7 were recorded using yellow food coloring dissolved into the stock media. Recorded data was inverted in post-processing to visualize the hyphae, pillar and channel. By adding this dye we were able to obtain three-dimensional time-lapse images of hyphae of *A. bisexualis* interacting with measurement pillars (see Suppl. for movie).

As can be observed from the cross-sections shown on the right of Fig. 7, force application by the hypha was limited to the x-y plane, with no deflection in the z-direction visible. Possible growth in the z-axis or a helical growth path of the tip was previously suggested and used as an argument against pulsatile growth in the x-axis in tip growing organisms [32]. However, it was argued that for this to be possible growth at inclinations of about 10 degrees to the horizontal would be necessary [33]. Such an inclination would result in hyphae moving out of the optical plane of focus within about 6 μm, which would be easily detectable in the confocal microscopy images.

Devices fabricated for use with the fungi *N. crassa* were employed to characterize protrusive force generation and correlations to the hyphal growth rate. Figure 8 shows the results of force measurements on twelve hyphae of *N. crassa*. Prior to force sensing, hyphae were observed using the 5 or 10x objective of a light microscope while they grew out from the seeding area into the measurement channels. In Fig. 8(a) *N. crassa* hyphae can be seen extending towards the channel inlets shortly after inoculation. Due to the transparent nature of the PDMS chips, hyphal parameters, such as width and growth rate, could be recorded and analyzed simultaneously to the force measurements. On average, we observed that *N. crassa* hyphae grew slower on the chips ($2.9 \pm 1.2\ \mu m/min$ (n = 20)) than on Petri dishes ($29.2 \pm 0.42\ \mu m/min$), a difference not observed for *A. bisexualis* hyphae. In other studies where *N. crassa* was grown on PDMS chips the fungus does

appear to be sensitive to the channel environment/parameters. Variable growth rates have been reported when hyphae were growing in very long channels [34] and there have been reports of a slower rate of growth for *N. crassa* in spiral channels compared to wider channels [35]. Clearly this is an area where further work is warranted.

Once hyphal tips grew to within approximately 50-100 μm of the measurement pillar, a 20x objective was used and the microscope was focused on the top of the pillar. The growth of hyphae contacting the force sensing pillars and the deflection of the free end of the pillars were recorded. Image sequences were imported into ImageJ and exported in 2D coordinate/time (X,Y,t) format of the position of the pillar top circle. Given a half-diameter contact height, both force magnitude and direction were calculated by a custom algorithm based on the model combining pure bending and shear of the imposed force to a cantilever beam [19]. An example output of the algorithm is shown in Fig. 8(b) with the red arrow indicating force direction and magnitude. Force values recorded at each time-point were plotted in x- and y-directions (Fig. 8(c)) and as the total force (Fig. 8(d)) as a function of time. The ability to track the direction of the force application was particularly useful, as, in the case of this work, the Fy-component corresponded to protrusive force generation in line with hyphal extension, while the Fx-component corresponded to a squeezing force perpendicular to extension. For the example hypha shown, the Fy-component initially increased to 0.5 μN and then reached a maximum of 11 μN. From the force vector plot in Fig. 8(d) it can be observed how the direction of the applied force changed while the hypha interacted with the pillar from initial contact to squeezing past it. This means that not only were protrusive force measurements using elastomeric micropillars demonstrated for *N. crassa* for the first time, but also that the platform enabled in-depth studies of hyphal-pillar interactions.

Due to the number of parallel channels included on each device and the ease of fabricating multiple devices by molding off of an existing mold, measurements could further be extended to multiple hyphae. Figure 8(e) shows the protrusive Fy-component exerted by a sample of twelve *N. crassa* hyphae plotted as a function of growth rate and hyphal diameter. The overall range of measured forces was comparable to those observed for larger *A. bisexualis* hyphae. Force magnitude did not increase with hyphal diameter or growth rate for these hyphae, which were selected as they impacted the force-sensing pillars directly with their tips. Data previously recorded for the oomycete *A. bisexualis* [20], showed the same correlation when side-impacting hyphae were excluded and only tip-impacting hyphae considered [36]. In summary, this data demonstrates that the platform has the potential to provide a new tool to help understand the molecular dynamics that underlie protrusive growth. We are currently using the devices to investigate the role the cytoskeleton and turgor pressure play in protrusive force generation. In the near future we are aiming to combine the platform with RootChip technology [37] to screen water-soluble compounds secreted inhibiting growth or sporulation and explore the potential for holobiont-based biocontrol strategies. We expect that, in the long run, the platform will help combat loss of biodiversity due to these organisms by assisting in the development of new antifungal drugs.

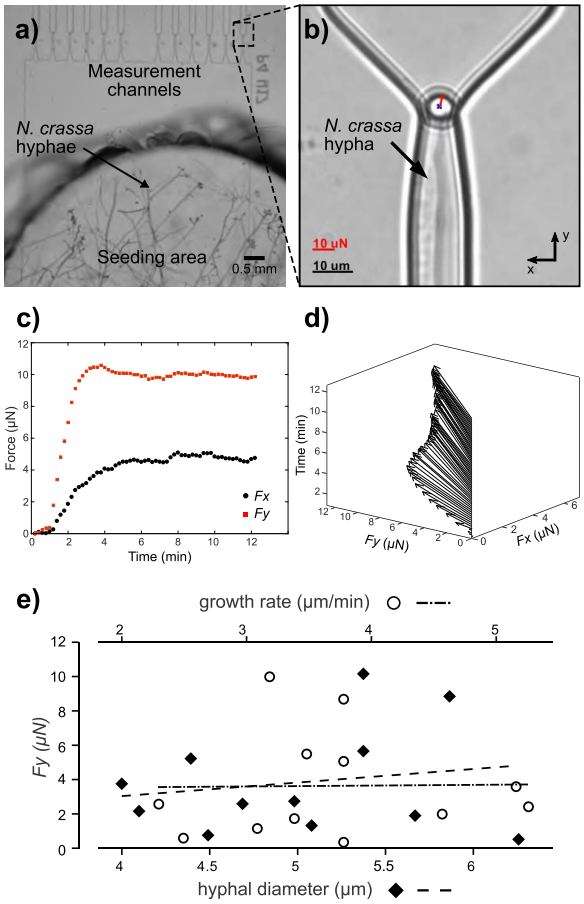

Fig. 8. Protrusive force measurements on hyphae of *N. crassa*. (a) Optical micrograph showing hyphae of *N. crassa* growing from the seeding area of the chip towards the measurement channels containing the sensor pillars. (b) Example image of the output generated by the image processing algorithm. The center of the pillar top is tracked and any translation in x,y-direction is converted into a force vector. This is overlaid onto the image in form of the arrow (red) originating from the pillar-top center, denoting force magnitude (arrow length) and direction (arrow angle) imparted on the pillar by the hypha growing from the bottom to the top. (c) Typical protrusive force plot showing the force imparted onto the pillar split into x- and y-direction components as a function of time. The Fy component is in-line with hypha extension and corresponds to the protrusive force. Hypha-pillar contact is typically characterized by a rapid onset of force, followed by a the hypha squeezing past the pillar, which is indicated by the later increase in Fx component. (d) Plot of the total force vector $F(x, y)$ as a function of time, demonstrating the platforms capability to visualize the directionality of force application. (e) Scatter plot of the protrusive force exerted by twelve *N. crassa* hyphae as a function of hyphal growth rate (○) and diameter (◆). The diameter was measured just prior to contact with the pillar and Fy two minutes after contact. Hyphae were selected to be hitting the pillar with the tip, as opposed to with their sides. A multi-linear regression analysis revealed no relationship between growth rate, diameter and force. Data were fitted with linear trend lines ($R^2 = 0.0002$ for growth rate and 0.01 for diameter).

IV. Conclusion

We have developed a lab-on-a-chip platform with single elastomeric micropillars in channel constrictions, which enabled the measurement of protrusive forces exerted by individual fungal hyphae. We introduced the device design and described optimizations of the fabrication process required to

adapt the microfluidic devices from wider oomycete hyphae to relatively thin fungal hyphae. The optimization of exposure dose for the novel positive photoresists, AZ 40XT and AZ 12XT, and negative resist AZ 15nXT enabled the production of monolithic elastomeric chips with individual high aspect-ratio micropillars inside microfluidic channels, a process which is likely to be useful for other force-sensing applications. We demonstrated the applicability of the platform by using it to perform confocal microscopy on the oomycete *A. bisexualis* while it interacted with and deflected a force measurement pillar. Moreover, we successfully cultured the fungi *N. crassa* on the platform and demonstrated the first measurements of protrusive forces exerted by individual hypha of this organism. The platform will help to extend the understanding of mechanisms that underlie invasive growth and pathogenicity of these microorganisms.

ACKNOWLEDGMENTS

The authors would like to thank Helen Devereux, Gary Turner and Kevin Stobbs for technical assistance.

REFERENCES

[1] Y. Sun, A. Tayagui, H. Shearer, A. Garrill, and V. Nock, "A microfluidic platform with integrated sensing pillars for protrusive force measurements on neurospora crassa," in *Proc. IEEE 31st Int. Conf. MEMS*, Belfast, U.K., Jan. 2018, pp. 1116–1119.

[2] M. C. Fisher *et al.*, "Emerging fungal threats to animal, plant and ecosystem health," *Nature*, vol. 484, no. 7393, pp. 186–194, 2012.

[3] R. A. Wilson and N. J. Talbot, "Under pressure: Investigating the biology of plant infection by *Magnaporthe oryzae*," *Nature Rev. Microbiol.*, vol. 7, pp. 185–195, Mar. 2009.

[4] M. C. Fisher, T. W. Garner, and S. F. Walker, "Global emergence of batrachochytrium dendrobatidis and amphibian chytridiomycosis in space, time, and host," *Ann. Rev. Microbiol.*, vol. 63, no. 1, pp. 291–310, 2009.

[5] M. C. Fisher, N. J. Hawkins, D. Sanglard, and S. J. Gurr, "Worldwide emergence of resistance to antifungal drugs challenges human health and food security," *Science*, vol. 360, no. 6390, pp. 739–742, 2018.

[6] M. Bastmeyer, H. B. Deising, and C. Bechinger, "Force exertion in fungal infection," *Ann. Rev. Biophys. Biomol. Struct.*, vol. 31, no. 1, pp. 321–341, 2002.

[7] N. P. Money, "Wishful thinking of turgor revisited: The mechanics of fungal growth," *Fungal Genet. Biol.*, vol. 21, no. 2, pp. 173–187, 1997.

[8] A. Muralidhar *et al.*, "A pressure gradient facilitates mass flow in the oomycete *Achlya bisexualis*," *Microbiology*, vol. 162, no. 2, pp. 206–213, 2016.

[9] S. Suei and A. Garrill, "An F-actin-depleted zone is present at the hyphal tip of invasive hyphae of *Neurospora crassa*," *Protoplasma*, vol. 232, nos. 3–4, pp. 72–165, 2008.

[10] A. S. Nezhad and A. Geitmann, "The cellular mechanics of an invasive lifestyle," *J. Exp. Botany*, vol. 64, no. 15, pp. 4709–4728, 2013.

[11] S. Johns, C. M. Davis, and N. P. Money, "Pulses in turgor pressure and water potential: Resolving the mechanics of hyphal growth," *Microbiol. Res.*, vol. 154, no. 3, pp. 225–231, 1999.

[12] A. S. Nezhad, "Microfluidic platforms for plant cells studies," *Lab Chip*, vol. 14, no. 17, pp. 3262–3274, 2014.

[13] C. E. Stanley, G. Grossmann, X. C. I. Solvas, and A. J. DeMello, "Soil-on-a-Chip: Microfluidic platforms for environmental organismal studies," *Lab Chip*, vol. 16, no. 2, pp. 228–241, 2016.

[14] N. Minc, A. Boudaoud, and F. Chang, "Mechanical forces of fission yeast growth," *Current Biol.*, vol. 19, no. 13, pp. 1096–1101, 2009.

[15] A. S. Nezhad, M. Naghavi, M. Packirisamy, R. Bhat, and A. Geitmann, "Quantification of the Young's modulus of the primary plant cell wall using bending-lab-on-chip (BLOC)," *Lab Chip*, vol. 13, no. 13, pp. 2599–2608, 2013.

[16] A. Ghanbari, V. Nock, S. Johari, R. Blaikie, X. Chen, and W. Wang, "A micropillar-based on-chip system for continuous force measurement of *C. elegans*," *J. Micromech. Microeng.*, vol. 22, no. 9, p. 095009, 2012.

[17] S. Johari, V. Nock, M. M. Alkaisi, and W. Wang, "On-chip analysis of *C. elegans* muscular forces and locomotion patterns in microstructured environments," *Lab Chip*, vol. 13, no. 9, pp. 1699–1707, 2013.

[18] V. Nock, A. Tayagui, and A. Garrill, "Elastomeric micropillar arrays for the study of protrusive forces in hyphal invasion," in *Proc. MicroTAS Conf.*, Gyeongju, South Korea, 2015, pp. 692–694.

[19] A. Tayagui, A. Garrill, D. Collings, and V. Nock, "On-chip measurement of protrusive force exerted by single hyphal tips of pathogenic microorganisms," in *Proc. MicroTAS Conf.*, Dublin, Ireland, 2016, pp. 150–151.

[20] A. Tayagui, Y. Sun, D. A. Collings, A. Garrill, and V. Nock, "An elastomeric micropillar platform for the study of protrusive forces in hyphal invasion," *Lab Chip*, vol. 17, no. 21, pp. 3643–3653, 2017.

[21] C. M. Roche, J. J. Loros, K. McCluskey, and N. L. Glass, "*Neurospora crassa*: Looking back and looking forward at a model microbe," *Amer. J. Botany*, vol. 101, no. 12, pp. 2022–2035, 2014.

[22] J. Schindelin *et al.*, "Fiji: An open-source platform for biological-image analysis," *Nature Methods*, vol. 9, no. 7, pp. 676–682, Jul. 2012.

[23] K. Nagayama, T. Inoue, Y. Hamada, and T. Matsumoto, "A novel patterned magnetic micropillar array substrate for analysis of cellular mechanical responses," *J. Biomech.*, vol. 65, pp. 194–202, Dec. 2017.

[24] J. C. Doll *et al.*, "SU-8 force sensing pillar arrays for biological measurements," *Lab Chip*, vol. 9, no. 10, pp. 1449–1454, 2009.

[25] N. Thanh-Vinh *et al.*, "High-sensitivity microelectromechanical systems-based tri-axis force sensor for monitoring cellular traction force," *IET Micro Nano Lett.*, vol. 11, no. 10, pp. 563–567, Oct. 2016.

[26] L. Yang, X. Hao, C. Wang, B. Zhang, and W. Wang, "Rapid and low cost replication of complex microfluidic structures with PDMS double casting technology," *Microsyst. Technol.*, vol. 20, nos. 10–11, pp. 1933–1940, 2014.

[27] M. J. Madou, *Fundamentals of Microfabrication: The Science of Miniaturization*, 2nd ed. New York, NY, USA: Taylor & Francis, 2002.

[28] S. K. Walker, K. Chitcholtan, Y. Yu, G. M. Christenhusz, and A. Garrill, "Invasive hyphal growth: An F-actin depleted zone is associated with invasive hyphae of the oomycetes *Achlya bisexualis* and *Phytophthora cinnamomi*," *Fungal Genet. Biol.*, vol. 43, no. 5, pp. 357–365, 2006.

[29] T. Ketelaar, H. J. G. Meijer, M. Spiekerman, R. Weide, and F. Govers, "Effects of latrunculin B on the actin cytoskeleton and hyphal growth in *Phytophthora infestans*," *Fungal Genet. Biol.*, vol. 49, no. 12, pp. 1014–1022, 2012.

[30] H. J. G. Meijer, C. Hua, K. Kots, T. Ketelaar, and F. Govers, "Actin dynamics in *Phytophthora infestans*; rapidly reorganizing cables and immobile, long-lived plaques," *Cellular Microbiol.*, vol. 16, no. 6, pp. 948–961, 2014.

[31] K. Kots, H. J. G. Meijer, K. Bouwmeester, F. Govers, and T. Ketelaar, "Filamentous actin accumulates during plant cell penetration and cell wall plug formation in *Phytophthora infestans*," *Cellular Mol. Life Sci.*, vol. 74, no. 5, pp. 909–920, 2017.

[32] S. L. Jackson, "Do hyphae pulse as they grow?" *New Phytol.*, vol. 151, no. 3, pp. 556–560, 2001.

[33] K. Sampson, R. R. Lew, and I. B. Heath, "Time series analysis demonstrates the absence of pulsatile hyphal growth," *Microbiology*, vol. 149, no. 11, pp. 3111–3119, 2003.

[34] T. Geng *et al.*, "Compartmentalized microchannel array for high-throughput analysis of single cell polarized growth and dynamics," *Sci. Rep.*, vol. 5, Nov. 2015, Art. no. 16111.

[35] K. K. Lee, L. Labiscsak, C. H. Ahn, and C. I. Hong, "Spiral-based microfluidic device for long-term time course imaging of *Neurospora crassa* with single nucleus resolution," *Fungal Genet. Biol.*, vol. 94, pp. 11–14, Sep. 2016.

[36] A. Tayagui, "Measurement of protrusive forces in hyphae using lab-on-a-chip technology," Ph.D. dissertation, Dept. Biol. Sci., Univ. Canterbury, Christchurch, New Zealand, 2018.

[37] G. Grossmann *et al.*, "The RootChip: An integrated microfluidic chip for plant science," *Plant Cell*, vol. 23, no. 12, pp. 4234–4240, 2011.

Yiling Sun received the bachelor's degree in biomedical engineering from the School of Medicine, Shanghai Jiao Tong University, China, in 2009, and the master's degree in micro-nano systems engineering from the Graduate School of Engineering, Nagoya University, Japan, in 2014. She is currently pursuing the Ph.D. degree with the Department of Electrical and Computer Engineering, University of Canterbury, New Zealand. Her research interests include microfabrication and Lab-on-a-Chip devices for use in biology.

Ayelen Tayagui received the Licentiate degree in genetics from the National University of Misiones in Argentina in 2010. She is currently pursuing the Ph.D. degree with the School of Biological Sciences, University of Canterbury, New Zealand. Her research interests include determining the role of the cytoskeleton plays in regulating protrusive forces in fungi and related organisms and how these forces might play a role in the pathogenicity of these organisms.

Ashley Garrill received the B.Sc. degree (Hons.) in genetics and plant biology from the University of Leeds in 1986 and the Ph.D. degree in genetics and microbiology from the University of Liverpool in 1990. He is currently an Associate Professor with the School of Biological Sciences, University of Canterbury. His research interests include the invasive growth of pathogenic microbes.

Volker Nock (M'05) is currently a Senior Lecturer with the Department of Electrical and Computer Engineering, University of Canterbury, New Zealand, where he is also a Co-Director of the Biomolecular Interactions Centre. He is also an Associate Investigator of the MacDiarmid Institute for Advanced Materials and Nanotechnology and the MedTech Centres of Research Excellence.

He received the Dipl.Ing. degree in microsystem technology from the Institute for Microsystem Technology, Albert-Ludwigs University of Freiburg, Germany, in 2005, and the Ph.D. degree in electrical and electronic engineering from the University of Canterbury, New Zealand, in 2009. His dissertation focused on the control and measurement of dissolved oxygen in microfluidic bioreactors. From 2009 to 2012, he was a MacDiarmid and Marsden Research Fellow at the Department of Electrical and Computer Engineering on Bioimprinting.

His research interests focus on microfabrication, materials, and microfluidic devices at the interface of biology, chemistry, and medicine. He is a member of the Royal Society of New Zealand.